

# COOPERATIVE JAHN-TELLER EFFECT ON THE MAGNETIC STRUCTURE OF MANGANESE OXIDES \*

Takashi Hotta, Seiji Yunoki, and Elbio Dagotto

National High Magnetic Field Laboratory  
Florida State University, Tallahassee, FL 32306

## Abstract

The magnetic structure of  $\text{LaMnO}_3$  is investigated on three-dimensional clusters of  $\text{MnO}_6$  octahedra by using a combination of relaxation and Monte Carlo techniques. It is found that the cooperative Jahn-Teller phonons lead to the stabilization of A-type anti-ferromagnetic and C-type orbital structures in the physically relevant region of parameter space for  $\text{LaMnO}_3$  with small corrections due to tilting effects. The results suggest that strong Coulomb interactions are not necessary for a qualitative description of undoped manganites. In fact, it is shown that the present result is not essentially changed even if the Coulomb interaction is explicitly included.

## 1 Introduction

The study of manganese oxides is receiving considerable attention in recent years both in its theoretical and experimental aspects [1]. From the technological viewpoint, these materials could be used in the preparation of high-sensitive magnetic-field sensors due to their colossal magnetoresistance (CMR) phenomena. In addition, researchers in the condensed matter field have been interested in the rich phase diagram of these materials originating from the competition and interplay among charge, spin, and orbital degrees of freedoms. Obtaining a unified picture for this rich phase diagram is a challenging open problem.

A prototype for the theoretical investigation of manganese oxides is the double-exchange (DE) framework, describing the hopping motion of  $e_g$ -electrons ferromagnetically coupled to localized  $t_{2g}$ -spins. This idea has conceptually explained the appearance of ferromagnetism when holes are doped [2]. In addition, within the one orbital model, the existence of phase separation has been recently unveiled with the use of modern numerical techniques [3], leading to a potential explanation of the CMR effect [4].

However, in order to understand the fine details of the phase diagram of manganites, the one-orbital model is not sufficient since the highly nontrivial A-type spin antiferro (AF)

---

\*To appear in proceedings of the conference “Science and Technology of Magnetic Oxides ’99”, La Jolla, July 5–7, 1999.

and C-type orbital structures observed experimentally in the undoped material  $\text{LaMnO}_3$ [5] cannot be properly addressed in such a simple context. Certainly two-orbital models are needed to consider the nontrivial state of undoped manganites. In this framework the two-band model without phonons has been studied before, and the importance of the strong Coulomb repulsion has been remarked for the appearance of the A-AF state [6, 7, 8, 9]. This is based upon the belief that the competition between kinetic and strong correlation effect determines the optimal orbital for  $e_g$ -electrons and the lattice will be simply distorted to reproduce such optimal orbitals. However, Coulombic approaches have presented conflicting results regarding the orbital order that coexists with the A-type spin state, with several approaches predicting G-type orbital order, which is not observed in practice.

While it is certainly correct that the orbital degrees of freedom play an essential role for the stabilization of A-AF, it should be noticed that our understanding is still incomplete. In particular, it is important to remark that the orbital structure is tightly related to the Jahn-Teller (JT) distortion of  $\text{MnO}_6$  octahedron. If each JT distortion would occur independently, optimal orbitals can be determined by minimizing the kinetic and interaction energy of  $e_g$ -electrons. However, oxygens are shared between adjacent  $\text{MnO}_6$  octahedra, indicating that the JT distortions occurs cooperatively. Especially in the undoped situation, all  $\text{MnO}_6$  octahedra exhibit JT distortion, indicating that the cooperative effect is very important, as discussed by Kanamori [10]. Thus, in order to understand the magnetic and orbital structures in  $\text{LaMnO}_3$ , it is indispensable to optimize simultaneously the electron and lattice systems. However, not much effort has been devoted to the microscopic treatment of the cooperative effect [11], although the JT effect in the manganese oxide has been studied by several groups [12, 13, 14, 15, 16]. Then, in the present work, a careful investigation of this problem is performed with some numerical techniques, focusing on  $n = 1$ , where  $n$  is the electron number per site.

In this paper, the optimal oxygen positions are determined by a relaxation technique to obtain the lattice distortions corresponding to several  $t_{2g}$ -spin magnetic structures. In addition, Monte Carlo (MC) simulations were also performed to investigate the spin and orbital structure without *a priori* assumptions for their order. It is found that A-AF, as well as the C-type orbital structure, occurs in realistic parameter regions for  $\text{LaMnO}_3$ , i.e., large Hund coupling between the  $e_g$ -electron and  $t_{2g}$ -spin, small AF interaction between  $t_{2g}$ -spins, and strong electron-lattice coupling. It should be emphasized that our results are obtained without the Coulomb interaction. It is shown in a simple case that the optimized results are essentially unchanged even if the Coulomb interaction is included explicitly in the model.

The organization of this paper is as follows. Section 2 is devoted to the formulation to include the cooperative effect in the two-orbital model tightly coupled to the JT distortion, and some technical points are briefly discussed. In Sec. 3, the results on the magnetic and orbital structures are provided and it is shown that the region of A-AF in the magnetic phase diagram is reasonable for  $\text{LaMnO}_3$ , since the couplings needed agree with experiments. In Sec. 4, a prescription to obtain the C-type orbital order with the alternation of  $3x^2 - r^2$  and  $3y^2 - r^2$  orbitals is provided. Finally, in Sec. 5, the effect of the Coulomb interaction on the lattice distortion is discussed in the ferromagnetic state. Throughout this paper, units such

that  $\hbar = k_B = 1$  are used.

## 2 Formulation

### 2.1 Hamiltonian

Let us consider the motion of  $e_g$ -electrons tightly coupled to the localized  $t_{2g}$ -spins and the local distortions of the  $\text{MnO}_6$  octahedra. This situation is well described by

$$H = H_{\text{2orb}} + H_{\text{AFM}} + H_{\text{el-ph}} + H_{\text{el-el}}. \quad (1)$$

Here the first term indicates the two-orbital Hamiltonian, given by,

$$H_{\text{2orb}} = - \sum_{\mathbf{i}\alpha\gamma\gamma'\sigma} t_{\gamma\gamma'}^{\mathbf{a}} c_{\mathbf{i}\gamma\sigma}^\dagger c_{\mathbf{i}+\mathbf{a}\gamma'\sigma} - J_H \sum_{\mathbf{i}\gamma\sigma\sigma'} \mathbf{S}_{\mathbf{i}} \cdot c_{\mathbf{i}\gamma\sigma}^\dagger \sigma_{\sigma\sigma'} c_{\mathbf{i}\gamma\sigma'}, \quad (2)$$

where  $c_{\mathbf{i}\alpha\sigma}$  ( $c_{\mathbf{i}\beta\sigma}$ ) is the annihilation operator for an  $e_g$ -electron with spin  $\sigma$  in the  $d_{x^2-y^2}$  ( $d_{3z^2-r^2}$ ) orbital at site  $\mathbf{i}$ . The vector connecting nearest-neighbor sites is  $\mathbf{a}$ ,  $t_{\gamma\gamma'}^{\mathbf{a}}$  is the hopping amplitude between  $\gamma$ - and  $\gamma'$ -orbitals connecting nearest-neighbor sites along the  $\mathbf{a}$ -direction via the oxygen  $2p$ -orbital,  $J_H$  is the Hund coupling,  $\mathbf{S}_{\mathbf{i}}$  the localized classical  $t_{2g}$ -spin normalized to  $|\mathbf{S}_{\mathbf{i}}| = 1$ , and  $\sigma = (\sigma_1, \sigma_2, \sigma_3)$  are the Pauli matrices.

The second term is needed to account for the AFM character of the manganese oxide, given by

$$H_{\text{AFM}} = J' \sum_{\langle \mathbf{i}, \mathbf{j} \rangle} \mathbf{S}_{\mathbf{i}} \cdot \mathbf{S}_{\mathbf{j}}, \quad (3)$$

where  $J'$  is the AF-coupling between nearest-neighbor  $t_{2g}$ -spins.

In the third term, the coupling of  $e_g$ -electrons to the distortion of  $\text{MnO}_6$  octahedron is considered as

$$\begin{aligned} H_{\text{el-ph}} &= g \sum_{\mathbf{i}\sigma\gamma\gamma'} c_{\mathbf{i}\gamma\sigma}^\dagger (Q_{1\mathbf{i}}\sigma_0 + Q_{2\mathbf{i}}\sigma_1 + Q_{3\mathbf{i}}\sigma_3)_{\gamma\gamma'} c_{\mathbf{i}\gamma'\sigma} \\ &+ (1/2) \sum_{\mathbf{i}} [k_{\text{br}} Q_{1\mathbf{i}}^2 + k_{\text{JT}} (Q_{2\mathbf{i}}^2 + Q_{3\mathbf{i}}^2)], \end{aligned} \quad (4)$$

where  $g$  is the electron-phonon coupling constant,  $Q_{1\mathbf{i}}$  denotes the distortion for the breathing mode of the  $\text{MnO}_6$  octahedron,  $Q_{2\mathbf{i}}$  and  $Q_{3\mathbf{i}}$  are, respectively, JT distortions for the  $(x^2 - y^2)$ - and  $(3z^2 - r^2)$ -type modes, and  $\sigma_0$  is the  $2 \times 2$  unit matrix. Spring constants for breathing- and JT-modes are denoted by  $k_{\text{br}}$  and  $k_{\text{JT}}$ , respectively.

The final term indicates the Coulomb interactions between  $e_g$ -electrons. As mentioned in Sec. 1, since only the JT phonons are investigated, the Coulomb interactions are neglected. This point will be discussed later in the text (Sec. 5) where the explicit form of  $H_{\text{el-el}}$  is provided and briefly analyzed.

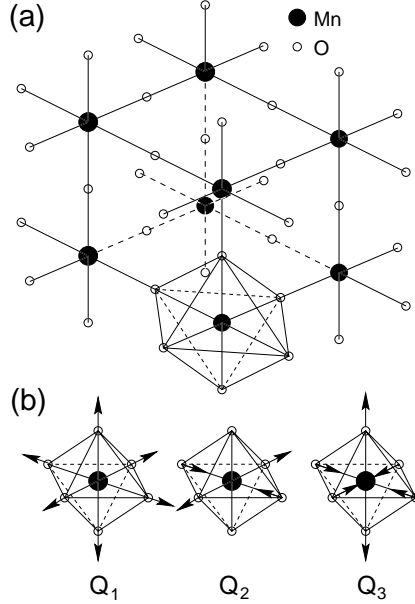


Figure 1: (a)  $2 \times 2 \times 2$  lattice composed of eight  $\text{MnO}_6$  octahedra. Note that oxygens are shared by adjacent octahedra. (b) Three kinds of distortions of octahedron considered in this paper. The arrows indicate the direction of displacement of oxygens.

## 2.2 Lattice distortion

As shown in Fig. 1(a), oxygens are shared between adjacent octahedra, indicating that the local lattice distortions cannot be treated independently and a cooperative analysis is needed for this problem. For this purpose, the normal coordinates for distortions of the  $\text{MnO}_6$  octahedron, shown in Fig. 1(b), are written as [11]

$$Q_{1i} = (1/\sqrt{3})(\Delta_{xi} + \Delta_{yi} + \Delta_{zi}), \quad (5)$$

for the breathing mode,

$$Q_{2i} = (1/\sqrt{2})(\Delta_{xi} - \Delta_{yi}), \quad (6)$$

and

$$Q_{3i} = (1/\sqrt{6})(2\Delta_{zi} - \Delta_{xi} - \Delta_{yi}), \quad (7)$$

for the JT modes, where  $\Delta_{ai}$  is given by

$$\Delta_{ai} = \Delta_a + \delta_{ai}. \quad (8)$$

The first term indicates the deviation from the cubic lattice, given by  $\Delta_a = L_a - L$ , where  $L_a$  is the length between Mn-ions along the  $\mathbf{a}$ -axis and  $L = (L_x + L_y + L_z)/3$ . The second term

is the contribution from the shift of oxygen position, expressed by  $\delta_{ai} = u_i^a - u_{i-a}^a$ , where  $u_i^a$  is the deviation of oxygen from the equilibrium position along the Mn-Mn bond in the  $\mathbf{a}$ -direction. By this consideration, the cooperative JT distortion as well as the macroscopic lattice deformation is reasonably taken into account. Note that the buckling and rotational modes of  $\text{MnO}_6$  octahedron are not explicitly included in this work. In general,  $L_{\mathbf{a}}$  can be different for each direction, depending on the bulk properties of the lattice. Since the present work focuses on the microscopic mechanism for A-AF formation in  $\text{LaMnO}_3$ , the undistorted lattice with  $L_x = L_y = L_z$  is treated first, and then corrections will be added.

### 2.3 Hopping amplitudes and energy scale

In the cubic undistorted lattice, the hopping amplitudes are given by [17]

$$t_{aa}^x = -\sqrt{3}t_{ab}^x = -\sqrt{3}t_{ba}^x = 3t_{bb}^x = t, \quad (9)$$

for the  $\mathbf{x}$ -direction,

$$t_{aa}^y = \sqrt{3}t_{ab}^y = \sqrt{3}t_{ba}^y = 3t_{bb}^y = t, \quad (10)$$

for the  $\mathbf{y}$ -direction, and

$$t_{bb}^z = 4t/3, t_{aa}^z = t_{ab}^z = t_{ba}^z = 0, \quad (11)$$

for the  $\mathbf{z}$ -direction. Throughout this paper, the energy unit is  $t$ .

Corresponding to this choice of the energy unit, the length in the lattice distortion is scaled by  $\sqrt{t/k_{\text{JT}}}$ . As a result of this scaling, a non-dimensional electron-phonon coupling constant  $\lambda$  is defined as

$$\lambda = g/\sqrt{k_{\text{JT}}t}. \quad (12)$$

It is noted that this coupling constant can be related to the static JT energy, which is conventionally defined by  $E_{\text{JT}} = g^2/(2k_{\text{JT}})$ , as

$$E_{\text{JT}} = t\lambda^2/2. \quad (13)$$

Note also that the present length scale is rewritten as

$$\sqrt{t/k_{\text{JT}}} = \ell_{\text{JT}}/\lambda, \quad (14)$$

where  $\ell_{\text{JT}} = g/k_{\text{JT}}$  is the characteristic length for the JT distortion. From the experimental result,  $\ell_{\text{JT}}$  is estimated as  $0.3\text{\AA}$  [5], which is a typical length in this context.

As for the spring constant for the breathing mode, it is expressed as  $k_{\text{br}} = \beta k_{\text{JT}}$  and the ratio  $\beta$  is treated as a parameter. If it is plausibly assumed that the reduced masses for those modes are equal, this ratio is given by  $\beta = (\omega_{\text{br}}/\omega_{\text{JT}})^2$ , where  $\omega_{\text{br}}$  and  $\omega_{\text{JT}}$  are the vibration energies for manganite breathing- and JT-modes, respectively. From experimental results and band-calculation data,  $\omega_{\text{br}}$  and  $\omega_{\text{JT}}$  are, respectively, estimated as  $\sim 700\text{cm}^{-1}$  and  $500\text{-}600\text{cm}^{-1}$  [18]. Then, throughout this work,  $\beta$  is taken as 2, although the results presented here are basically unchanged as long as  $\beta$  is larger than unity.

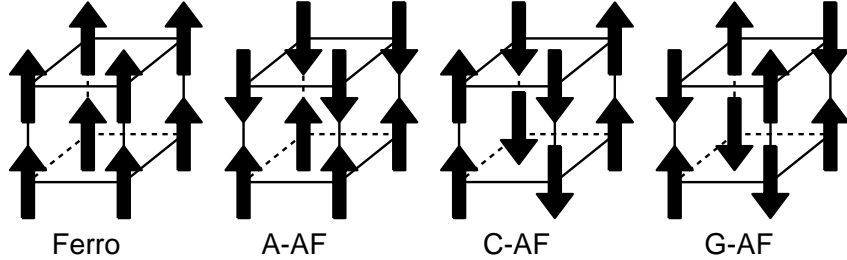


Figure 2: Magnetic structures in  $2 \times 2 \times 2$  clusters.

In this work, the change in  $t$  due to the displacement of oxygen position is not taken into account, but such an effect is shown to be very small as follows. Due to the pseudo-potential theory [19], the exact hopping amplitude, for example, along the  $\mathbf{x}$ -direction between a-orbitals in  $\mathbf{i}$  and  $\mathbf{i} + \mathbf{x}$  sites, is expressed as

$$t_{aa}^x = \frac{t}{(1 - \epsilon^2)^{7/2}}, \quad (15)$$

with  $\epsilon = |2u_i^x|/L_x$ . It should be remarked that the change in  $t_{aa}^x$  due to the oxygen shift is of the order of  $\epsilon^2$ , not of the order of  $\epsilon$ . Since  $\epsilon$  is estimated to be at most a few percent, the change is considered to be negligible. Thus, in the present work, such a change is not included to avoid unnecessary complication in the calculation. However, when the distorted lattice is considered, namely, when the deviation from  $L_x = L_y = L_z$  is taken into account, the change in the hopping matrix due to this distortion should be included, because the effect is of the order of  $\Delta_a/L$  in this case, not of the order of  $(\Delta_a/L)^2$ . This point will be discussed again in Sec. 4.

## 2.4 Techniques

To study Hamiltonian Eq. (1) without  $H_{\text{el-el}}$ , two numerical techniques have been applied. One is the relaxation technique, in which the optimal positions of the oxygens are determined by minimizing the total energy. In this calculation, only the stretching mode for the octahedron, is taken into account. Moreover, the relaxation has been performed for fixed structures of the  $t_{2g}$ -spins such as ferro (F), A-type AF (A-AF), C-type AF (C-AF), and G-type AF (G-AF), shown in Fig. 2. The advantage of this method is that the optimal orbital structure can be rapidly obtained on small clusters. However, the assumptions involved in the relaxation procedure should be checked with an independent method.

Such a check is performed with the unbiased MC simulations used before for one- and two-dimensional clusters using non-cooperative JT-phonons [15]. The dominant magnetic and

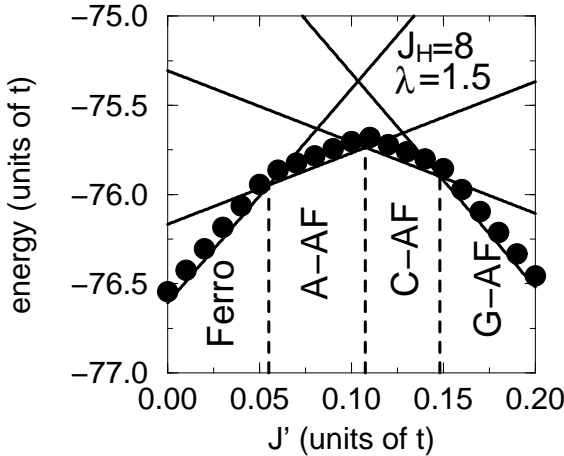


Figure 3: Total energy as a function of  $J'$  on a  $2 \times 2 \times 2$  lattice with  $J_H = 8$  and  $\lambda = 1.5$ . The solid lines and circles indicate the relaxation and MC results, respectively. MC simulations have been performed at temperature 1/200.

orbital structures are deduced from correlation functions. In the MC method, the clusters currently reachable are  $2 \times 2 \times 2$ ,  $4 \times 4 \times 2$ , and  $4 \times 4 \times 4$ . In spite of this size limitation, arising from the large number of degrees of freedom in the problem, the available clusters are sufficient for our mostly qualitative purposes. In addition, the remarkable agreement between MC and relaxation methods lead us to believe that our results are representative of the bulk limit.

### 3 Results

#### 3.1 Magnetic structure

In Fig. 3, the mean-energy is presented as a function of  $J'$  for  $J_H = 8$  and  $\lambda = 1.5$ , on a  $2 \times 2 \times 2$  cluster with open boundary conditions. The solid lines and symbols indicate the results obtained with the relaxation technique and MC simulations, respectively. The agreement is excellent, showing that the relaxation method is accurate. The small deviations between the results of the two techniques are caused by temperature effects. As intuitively expected, with increasing  $J'$  the optimal magnetic structure changes from ferro- to antiferromagnetic, and this occurs in the order  $F \rightarrow A\text{-AF} \rightarrow C\text{-AF} \rightarrow G\text{-AF}$ .

To check size effects, the  $t_{2g}$ -spin correlation function  $S(\mathbf{q})$  was calculated also in  $4 \times 4 \times 2$  and  $4 \times 4 \times 4$  clusters, where

$$S(\mathbf{q}) = (1/N) \sum_{i,j} e^{-i\mathbf{q} \cdot (i-j)} \langle \mathbf{S}_i \cdot \mathbf{S}_j \rangle. \quad (16)$$

Here  $N$  is the number of sites and  $\langle \dots \rangle$  indicates the thermal average value. As shown in Fig. 4, with increasing  $J'$  the dominant correlation changes in the order of  $\mathbf{q} = (0, 0, 0)$ ,

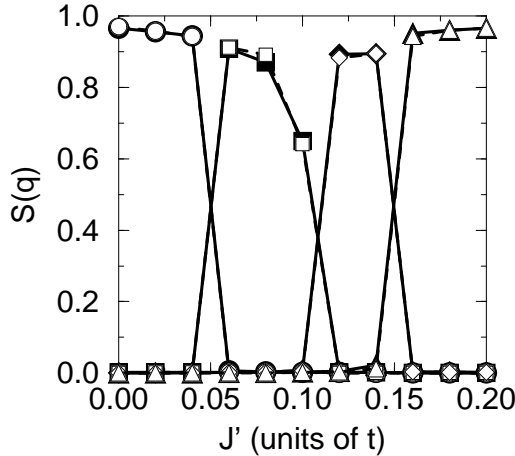


Figure 4: Spin correlation function  $S(\mathbf{q})$  obtained by MC simulations as a function of  $J'$ , at  $J_H = 8$  and  $\lambda = 1.5$ . Solid and open symbols denote the results in  $4 \times 4 \times 2$  and  $4 \times 4 \times 4$  clusters, respectively. Circles, squares, diamonds, and triangles indicates  $S(\mathbf{q})$  for  $\mathbf{q} = (0, 0, 0)$ ,  $(\pi, 0, 0)$ ,  $(\pi, \pi, 0)$ , and  $(\pi, \pi, \pi)$ , respectively.

$(\pi, 0, 0)$ ,  $(\pi, \pi, 0)$ , and  $(\pi, \pi, \pi)$ . The values of  $J'$  at which the spin structures changes agree well with those in Fig. 3.

### 3.2 Orbital structure

The shapes of the occupied orbital arrangement with the lowest energy for F, A-AF, C-AF, and G-AF magnetic structures are shown in Fig. 5. For the F-case, the G-type orbital structure is naively expected, because it is believed that the ferromagnetic spin structure is favored by the AF orbital configuration. However, a more complicated orbital structure is stabilized in the actual calculation, indicating the importance of the cooperative treatment for JT-phonons. For the A-AF state, only the C-type structure is depicted in Fig. 5, but the G-type structure, obtained by a  $\pi/2$ -rotation of the upper  $x$ - $y$  plane of the C-type state, was found to have *exactly* the same energy. Small corrections will remove this degeneracy in favor of the C-type as described in the next section. For C- and G-AF, the obtained orbital structures are G- and C-types, respectively.

Note that there exists an additional triplet degeneracy in the A-type state due to the cubic symmetry for each magnetic structure: If axes are changed cyclically ( $x \rightarrow y, y \rightarrow z, z \rightarrow x$ ), the optimized orbital structure is also transformed by this cyclic change, but the energy is invariant. Then, the magnetic and orbital structure in  $\text{LaMnO}_3$  occurs through a *spontaneous* symmetry breaking process.

Although the same change of the magnetic structure due to  $J'$  was already reported in the electronic model with purely Coulomb interactions [9], the orbital structures in those previous calculations were G-, G-, A-, and A-type for the F-, A-AF, C-AF, and G-AF spin states, respectively. Note that for the A-AF state, of relevance for the undoped manganites,

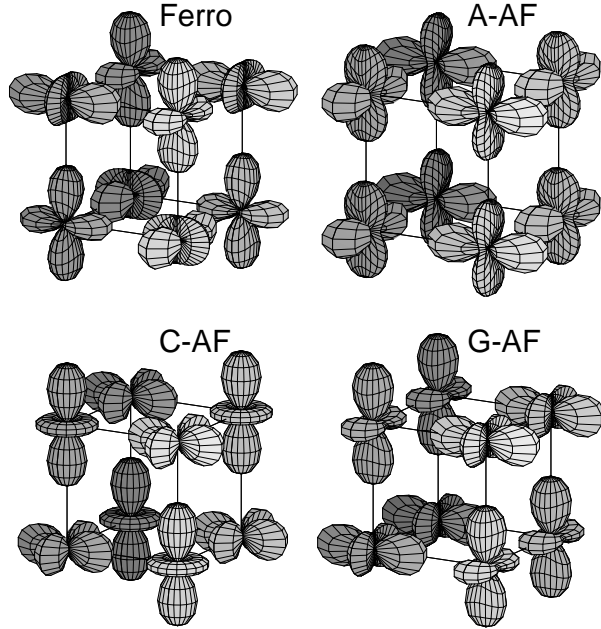


Figure 5: Optimized orbital structure for each magnetic structure.

the G-type order was obtained [9], although in another treatment for the Coulomb interaction, the C- and G-type structures were found to be degenerate [7], as in our calculation. Thus, the stabilization in experiments of the C-type orbital structure is still puzzling both in the JT and Coulomb mechanisms. This point will be discussed later in the text.

### 3.3 Magnetic phase diagram

In Figs. 6(a) and (b), the phase diagrams on the  $(J', \lambda)$ -plane are shown for  $J_H = 4$  and 8, respectively. The curves are drawn by the relaxation method. As expected, the F-region becomes wider with increasing  $J_H$ . When  $\lambda$  is increased at fixed  $J_H$ , the magnetic structure changes from F  $\rightarrow$  A-AF  $\rightarrow$  C-AF  $\rightarrow$  G-AF. This tendency is qualitatively understood if the two-site problem is considered in the limit  $J_H \gg 1$  and  $E_{JT} \gg 1$ . The energy-gain due to the second-order hopping process of  $e_g$ -electrons is roughly  $\delta E_{AF} \sim 1/J_H$  and  $\delta E_F \sim 1/E_{JT}$  for AF- and F-spin pairs, respectively. Increasing  $E_{JT}$ ,  $\delta E_F$  decreases, indicating the relative stabilization of the AF-phase. In our phase diagram, the A-AF phase appears for  $\lambda \geq 1.1$  and  $J' \leq 0.15$ . This region does not depend much on  $J_H$ , as long as  $J_H \gg 1$ . Although  $\lambda$  seems to be large, it is realistic from an experimental viewpoint:  $E_{JT}$  is 0.25eV from photoemission experiments [20] and  $t$  is estimated as  $0.2 \sim 0.5$ eV [21], leading to  $1 \leq \lambda \leq 1.6$ . As for  $J'$ , it

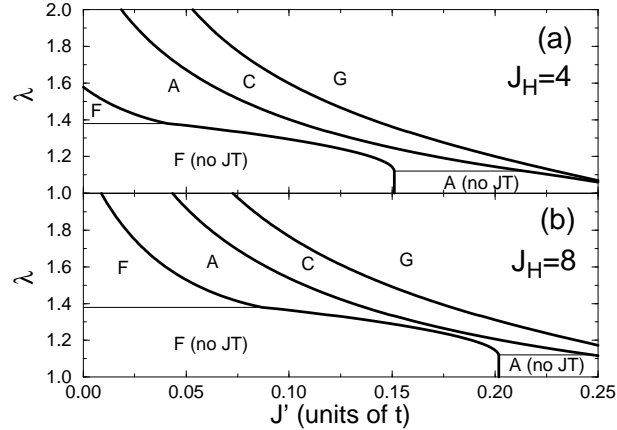


Figure 6: Magnetic phase diagram on the  $(J', \lambda)$  plane for (a)  $J_H = 4$  and (b) 8 (relaxation method). Below the thin solid lines in the F and A-AF regions, the JT-distortion disappears, suggesting that the system becomes metallic.

is estimated as  $0.02 \leq J' \leq 0.1$  [8, 22]. Thus, the location in parameter-space of the A-AF state found here is reasonable when compared with experimental results for LaMnO<sub>3</sub>.

## 4 Orbital order in the A-AF phase

Let us now focus on the orbital structure in the A-AF phase. In the cubic lattice studied thus far, the C- and G-type orbital structures are degenerate, and it is unclear whether the orbital pattern in the  $x$ - $y$  plane corresponds to the alternation of  $3x^2 - r^2$  and  $3y^2 - r^2$  orbitals observed in experiments [5]. To remedy the situation, some empirical facts observed in manganites become important: (i) The MnO<sub>6</sub> octahedra are slightly tilted from each other, leading to modifications in the hopping matrix. Among these modifications, the generation of a non-zero value for  $t_{aa}^z$  is important. (ii) The lattice is not cubic, but the relation  $L_{\text{in}} > L_{\text{out}}$  holds, where  $L_{\text{in}} = L_x = L_y$  and  $L_{\text{out}} = L_z$ . From experimental results [5], these numbers are estimated as  $L_{\text{in}} = 4.12\text{\AA}$  and  $L_{\text{out}} = 3.92\text{\AA}$ , indicating that the distortion with  $Q_3$ -symmetry occurs spontaneously.

For the inclusion of the point (ii),  $Q_{3i}$  in Eq. (7) is rewritten as

$$Q_{3i} = Q_3^{(0)} + (1/\sqrt{6})(2\delta_{zi} - \delta_{xi} - \delta_{yi}), \quad (17)$$

where  $Q_3^{(0)}$  indicates the spontaneous distortion with  $Q_3$ -symmetry, given by

$$Q_3^{(0)} = \sqrt{2/3}(L_{\text{out}} - L_{\text{in}}). \quad (18)$$

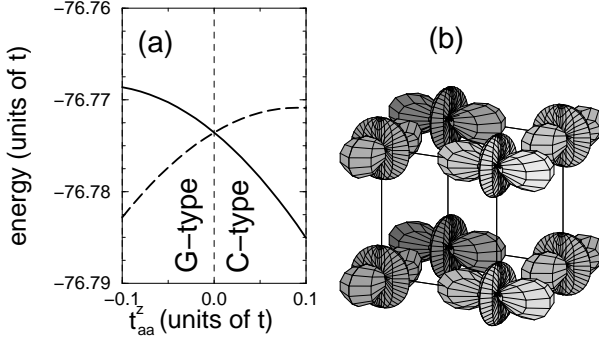


Figure 7: (a) Total energy as a function of  $t_{aa}^z$  on the  $2 \times 2 \times 2$  lattice with  $L_x = L_y > L_z$  for  $J_H = 8$ ,  $\lambda = 1.6$  and  $J' = 0.05$  (relaxation method). The solid and dashed curves denote the C- and G-orbital states, respectively. (b) Orbital structure in the A-AF phase for  $t_{aa}^z = 0^+$  and  $L_x = L_y > L_z$ . These shapes are very close to purely  $3x^2 - r^2$  and  $3y^2 - r^2$  types.

This length is rewritten in the non-dimensional form as  $Q_3^{(0)} = -\eta\lambda$ , where  $\eta$  is a numerical factor given by  $\eta = \sqrt{2/3}(L_{\text{in}} - L_{\text{out}})/\ell_{\text{JT}}$ , estimated as 0.5 by using the experimental data. Note that the hopping amplitude becomes different from those in the  $x$ - $y$  plane due to this distortion. As discussed shortly in subsection 2.3, it is obtained as  $t_{bb}^z = (4t/3)(L_{\text{in}}/L_{\text{out}})^7$ . As for  $J'$  along the  $z$ -direction, it is given by  $J'(L_{\text{in}}/L_{\text{out}})^{14}$ , since the superexchange interaction is proportional to the square of the hopping amplitude.

Motivated by these observations, the energies for C- and G-type orbital structures were recalculated including this time a nonzero value for  $t_{aa}^z$  in the magnetic A-AF state (see Fig. 7a)). In Fig. 8, the configuration of  $x^2 - y^2$  orbitals is depicted. From this figure, it is intuitively understood that if the  $x^2 - y^2$  orbitals in the upper and lower planes are tilted from the  $x$ - $y$  plane as showing by arrows in the figure, there appears finite a hopping integral between adjacent  $x^2 - y^2$  orbitals along the  $z$ -direction and the sign of this hopping amplitude is the same as that of  $t_{aa}^x$  or  $t_{aa}^y$ . Thus, in the real material, the tilting of the MnO<sub>6</sub> octahedra will always lead to a *positive* value for  $t_{aa}^z$  and the results of Fig. 7(a) suggest that the C-type orbital structure should be stabilized in the real materials. The explicit shape of the occupied orbitals is shown in Fig. 7(b). The experimentally relevant C-type structure with the approximate alternation of  $3x^2 - r^2$  and  $3y^2 - r^2$  orbitals is indeed successfully obtained by this procedure. Although the octahedron tilting actually leads to a change of all hopping amplitudes, effect not including in this work, the present analysis is sufficient to show that the C-type orbital structure is stabilized in the A-AF magnetic phase when  $t_{aa}^z$  is a small positive number, as it occurs in the real materials. Our investigations show that this mechanism to stabilize the C-type structure works also for the purely electronic model in the Hartree-Fock approximation.

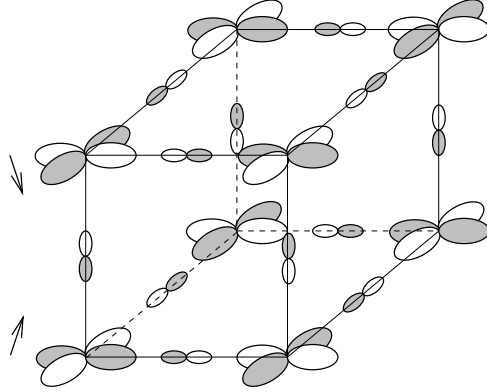


Figure 8: Configuration of  $x^2 - y^2$  orbitals connected by oxygen 2p orbitals in a  $2 \times 2 \times 2$  cluster. The open and hatched parts indicate the plus and minus sign in the orbitals, respectively. Arrows indicate the direction of the tilting.

## 5 Discussion and Summary

In this work, the Coulomb interaction term  $H_{\text{el-el}}$  has been neglected, but this detail needs further clarification. For this purpose,  $H_{\text{el-el}}$  is written as

$$H_{\text{el-el}} = U \sum_{\mathbf{i}\gamma} n_{\mathbf{i}\gamma\uparrow} n_{\mathbf{i}\gamma\downarrow} + U' \sum_{\mathbf{i}\sigma\sigma'} n_{\mathbf{i}\mathbf{a}\sigma} n_{\mathbf{i}\mathbf{b}\sigma'} + J \sum_{\mathbf{i}\sigma\sigma'} c_{\mathbf{i}\mathbf{a}\sigma}^\dagger c_{\mathbf{i}\mathbf{b}\sigma'}^\dagger c_{\mathbf{i}\mathbf{a}\sigma'} c_{\mathbf{i}\mathbf{b}\sigma}, \quad (19)$$

where  $U$  is the intra-orbital Coulomb interaction,  $U'$  the inter-orbital Coulomb interaction, and  $J$  is the inter-orbital exchange interaction. For Mn-oxides, they are estimated as  $U = 7\text{eV}$ ,  $J = 2\text{eV}$ , and  $U' = 5\text{eV}$  [8], which are large compared to  $t$ . However, the result for the optimized distortion described in this paper, obtained without the Coulomb interactions, is not expected to change, since the energy gain due to the JT-distortion is maximized when a single  $e_g$ -electron is present per site. This is essentially the same effect as produced by a short-range repulsion. In fact, the MC simulations show that the probability of double occupancy of a single orbital is negligible in the window of couplings where the A-type spin and C-type orbital state is stable.

In order to confirm the above statement, the JT- and breathing-distortions were calculated as a function of  $U'$  by using the Exact Diagonalization method on a  $2 \times 2$  cluster in the F-state in which  $U$  and  $J$  can be neglected. The result is shown in Fig. 9, where  $Q_{\text{JT}}$  and  $Q_{\text{br}}$  are defined as

$$Q_{\text{JT}} = (1/N) \sum_{\mathbf{i}} \sqrt{Q_{2\mathbf{i}}^2 + Q_{3\mathbf{i}}^2}, \quad (20)$$

and

$$Q_{\text{br}} = (1/N) \sum_{\mathbf{i}} |Q_{1\mathbf{i}}|, \quad (21)$$

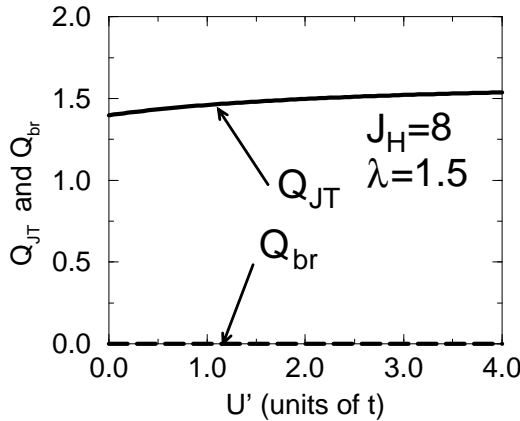


Figure 9: Mean-value of the breathing- and JT-mode distortions as a function of  $U'$  for the F-phase on a  $2 \times 2$  cluster for  $J_H = 8$  and  $\lambda = 1.5$ .

respectively. As expected, the mean value of the breathing-mode distortion is almost zero and only the JT-mode is active in the case of  $\beta = 2$ . It is noted that the dependence of  $Q_{JT}$  on  $U'$  is very weak, indicating that the optimized distortion is not affected by the Coulomb interaction. The orbital arrangement in this  $2 \times 2$  lattice is exactly the same as that in the  $x$ - $y$  plane of the orbital structure for the A-AF phase in Fig. 5 and this arrangement is unchanged by the inclusion of  $U'$ . Note also that  $Q_{JT}$  is gradually increased with the increase of  $U'$ , although the dependence is weak. This suggests that the JT-distortion without  $U'$  is reproduced at smaller value of  $\lambda$  if  $U'$  is included explicitly [16]. Thus, it is expected that the A-AF state will be stabilized at smaller  $\lambda$  improving the comparison of our results with experiments. Based on all these observations, it is believed that the effect of the Coulomb interaction is not crucial for the appearance of the A-AF state with the proper orbital order. Another way to rationalize this result is that the integration of the JT-phonons at large  $\lambda$  will likely induce Coulombic interactions dynamically.

Finally, let us briefly discuss transitions induced by the application of external magnetic fields on undoped manganites. When the A-AF state is stabilized, the energy difference (per site) obtained in our study between the A-AF and F states is about  $t/100$ . As a consequence, magnetic fields of  $20 \sim 50$ T could drive the transition from A-AF to F order accompanied by a change of orbital structure, interesting effect which may be observed in present magnetic field facilities.

In summary, with the use of numerical techniques at  $n = 1$ , it has been shown that the A-AF state is stable in models with JT-phonons, using coupling values physically reasonable for  $\text{LaMnO}_3$ . Our results indicate that it is not necessary to include large Coulombic interactions in the calculations to reproduce experimental results for the manganites. Considering the small but important effect of the octahedra tilting of the real materials, the C-type orbital structure (with the alternation pattern of  $3x^2 - r^2$  and  $3y^2 - r^2$  orbitals) has been successfully

reproduced for the A-AF phase in this context.

## Acknowledgments

T.H. is grateful to Y. Takada and H. Koizumi for enlightening discussion. T.H. is supported from the Ministry of Education, Science, Sports, and Culture of Japan. E.D. is supported by grant NSF-DMR-9814350.

## References

- [1] Jin *et al.*, Science **264**, 413 (1994); Y. Tokura *et al.*, J. Appl. Phys. **79**, 5288 (1996); A. P. Ramirez, J. Phys.: Condens. Matter **9**, 8171 (1997); Y. Tokura, in *Colossal Magnetoresistance Oxides*, ed. Y. Tokura, Gordon & Breach, Monographs in Cond. Matt. Science (1999).
- [2] C. Zener, Phys. Rev. **82**, 403 (1951); P. G. de Gennes, Phys. Rev. **118**, 141 (1960); P. W. Anderson and H. Hasegawa, Phys. Rev. **100**, 675 (1955).
- [3] S. Yunoki *et al.*, Phys. Rev. Lett. **80**, 845 (1998).
- [4] A. Moreo *et al.*, Science **283**, 2034 (1999).
- [5] E. O. Wallan and W. C. Koeler, Phys. Rev. **100**, 545 (1955); G. Matsumoto, J. Phys. Soc. Jpn. **29**, 606 (1970); J. B. A. Ellemaans *et al.*, J. Solid State Chem. **3**, 238 (1971). The C-type orbital structure has been recently confirmed with the use of high resolution X-ray diffraction technique (Y. Murakami *et al.*, Phys. Rev. Lett. **81**, 582 (1998)).
- [6] L. M. Roth, Phys. Rev. **141**, 306 (1966); K. I. Kugel and D. I. Khomskii, Usp. Fiz. Nauk. **136**, 621 (1981)[Sov. Phys. USP. **25**, 231 (1982)]; S. Inagaki, J. Phys. Soc. Jpn. **39**, 596 (1975); M. Cyrot and C. Lyon-Caen, J. Physique **36**, 253 (1975); W. Koshibae *et al.*, J. Phys. Soc. Jpn. **66**, 957 (1997); R. Shiina *et al.*, J. Phys. Soc. Jpn. **68**, 3159 (1997); L. F. Feiner and A. M. Oleś, Phys. Rev. B**59**, 3295 (1999); J. van den Brink *et al.*, Phys. Rev. B**59**, 6795 (1999).
- [7] T. Mizokawa and A. Fujimori, Phys. Rev. B**51**, 12880 (1995); *ibid* **54**, 5368 (1996).
- [8] S. Ishihara *et al.*, Phys. Rev. B**55**, 8280 (1997).
- [9] R. Maezono *et al.*, Phys. Rev. B**57**, R13993 (1998).
- [10] J. Kanamori, J. Appl. Phys. **31**, S14 (1960).
- [11] P. B. Allen and Vasili Perebeinos, cond-mat/9811250 and references therein.

- [12] I. Solovyev *et al.*, Phys. Rev. Lett. **76**, 4825 (1996); W. E. Pickett and D. J. Singh, Phys. Rev. B**53**, 1146 (1996).
- [13] A. J. Millis *et al.*, Phys. Rev. Lett. **74**, 5144 (1995); H. Röder *et al.*, Phys. Rev. Lett. **76**, 1356 (1996); A. J. Millis *et al.*, Phys. Rev. Lett. **77**, 175 (1996); A. J. Millis, *et al.*, Phys. Rev. B **54**, 5389; *ibid* 5405 (1996); D. Feinberg *et al.*, Phys. Rev. B**57**, R5583 (1998).
- [14] H. Koizumi *et al.*, Phys. Rev. Lett. **80**, 4518 (1998).
- [15] S. Yunoki *et al.*, Phys. Rev. Lett. **81**, 5612 (1998).
- [16] P. Benedetti and R. Zeyher, Phys. Rev. B**59**, 9923 (1999).
- [17] J. C. Slater and G. F. Koster, Phys. Rev. **94**, 1498 (1954).
- [18] M. N. Iliev *et al.*, Phys. Rev. B**57**, 2872 (1998).
- [19] W. A. Harrison, in *Electronic Structure and the Properties of Solids, The Physics of the Chemical Bond* (Freeman, San Francisco, 1980).
- [20] D. S. Dessau and Z.-X. Shen, in *Colossal Magnetoresistance Oxides*, ed. Y. Tokura, Gordon & Breach, Monographs in Cond. Matt. Science (1999).
- [21] A. E. Bacquet *et al.*, Phys. Rev. B**46**, 3771 (1992); A. Chainani, *et al.*, Phys. Rev. B**47**, 15397 (1993); T. Arima *et al.*, Phys. Rev. B**48**, 17006 (1993); T. Saito *et al.*, Phys. Rev. B**51**, 13942 (1995).
- [22] T. G. Perring *et al.*, Phys. Rev. Lett. **78**, 3197 (1997).